Article

Inverse Multiquadric Function to Price Financial Options under the Fractional Black–Scholes Model

Yanlai Song [1],* and Stanford Shateyi [2],*

1   College of Science, Zhongyuan University of Technology, Zhengzhou 450007, China
2   Department of Mathematics and Applied Mathematics, School of Mathematical and Natural Sciences, University of Venda, P. Bag X5050, Thohoyandou 0950, South Africa
*   Correspondence: 6392@zut.edu.cn (Y.S.); stanford.shateyi@univen.ac.za (S.S.)

Abstract: The inverse multiquadric radial basis function (RBF), which is one of the most important functions in the theory of RBFs, is employed on an adaptive mesh of points for pricing a fractional Black–Scholes partial differential equation (PDE) based on the modified RL derivative. To solve this problem, discretization along space is carried out on a non-uniform grid in order to focus on the hot area, at which the initial condition of the pricing model, i.e., the payoff, has discontinuity. The L1 scheme having the convergence order $2 - \alpha$ is used along the time fractional variable. Then, our proposed numerical method is built by matrices of differentiations to be as efficient as possible. Computational pieces of evidence are brought forward to uphold the theoretical discussions and show how the presented method is efficient in contrast to the exiting solvers.

Keywords: fractional Black–Scholes model; Caputo fractional derivative; radial basis function; memory; option pricing

MSC: 35R11; 91B74; 65M22

1. Introductory Notes and Preliminaries

The most fundamental option pricing model is the Black–Scholes (BS) partial differential equation (PDE), while many works have been introduced to overcome its shortcomings such as the Heston model with stochastic volatility, (see e.g., [1] and ([2] chapter 7)). Clearly, by generalizing the model for option pricing more assumptions have been relaxed, which has yielded more complicated forms of the model.

On the other hand, by increasing applications of fractional differential equations (FDEs) and keeping the memory feature for modeling, Wyss, in [3], investigated a tempered-fractional BS equation to evaluate European call options. The improved BS model with a fractional derivative actually comes from the fractional Brownian motion (FBM) with the real-valued Hurst exponent $0 < H < 1$, which is an exponent describing the memory of time series [4].

In fact, fractional stochastic differential equations (SDEs), as a generalization of Itô SDEs, require a considerable load of analytical challenges to obtain a solution [5,6]. However, this should be pursued because the volatility of stock-exchange variations could suitably be showed by a time variation of order $(dt)^H$. In spite of having attractive properties of the fractional BS model for the stock price, dealing with the FBM and its option pricing PDE formulation is challenging. In fact, there is some evidence that certain stock returns may exhibit the phenomenon of long memory (slowly decreasing covariance between returns at different times) [7], though this seems to be fairly weak. It is also generally accepted that stock returns display the phenomenon of clustering. None of these phenomena appear in semi-martingale models, such as the classic BS model. They do appear, however, if we consider the analogue of the BS model based on FBM with Hurst index H.

This superiority of the improved model under the fractional sense made researchers focus more on this model in practice.

Let $v(S_t, t)$ be a contingent payoff's price of $v(S_T, T)$ that is valid at the maturity $T > 0$. Considering the rate of interest r to be deterministic and under a fundamental martingale to produce an arbitrage-free option price [8], one is able to obtain the following forward in time pricing formula [3,9]:

$$\frac{\partial^\alpha v(s,\tau)}{\partial \tau^\alpha} = \frac{1}{2}\sigma^2 s^2 \frac{\partial^2 v(s,\tau)}{\partial s^2} + (r-q)s\frac{\partial v(s,\tau)}{\partial s} - rv(s,\tau), \qquad s \geq 0, \tag{1}$$

wherein $\tau = T - t$ is the time to maturity and the derivative is provided based on the (right) modified Riemann–Liouville (RL) derivative for $0 < \alpha \leq 1$. For $\alpha = 2H = 1$, viz., $H = 1/2$, (1) reduces to the classical BS equation. Moreover, σ, s, r and q stand for the volatility constant; the asset price; the riskless interest rate, which differs from country to country; and the dividend yield, respectively. Here, the transformation $\tau = T - t$ comes mainly from the fact the original financial PDE is backward in time after imposing the Itô lemma on the fractional SDE problem. Then, to transform it in order to have a forward in time PDE model, this transformation is employed.

The difference between call and put cases for vanilla options can be provided via their following payoffs ([2] chapter 1), respectively,

$$v(s,0) = \max\{0, s - E\}, \tag{2}$$

and

$$v(s,0) = \max\{0, E - s\}, \tag{3}$$

wherein the strike price is E.

For the European call and put options, the boundary conditions are defined, respectively, as follows [10]:

$$v(0,\tau) = 0, \ \lim_{s\to\infty} v(s,\tau) = s_{\max}\exp(-q\tau) - E\exp(-r\tau), \tag{4}$$

$$v(0,\tau) = E\exp\{-r\tau\}, \ \lim_{s\to\infty} v(s,\tau) = 0. \tag{5}$$

The introduction of the fractional derivative in (1) furnishes a long-memory feature for the returns. In fact, Lo, in [11], indicated that long-memory components in asset returns are crucial to many paradigms of modern financial economics.

It is necessary now to recall the definition of the modified RL derivative. Suppose that f is a real-valued continuous function; then, the modified RL fractional derivative is provided by [12]:

$$f^{(\alpha)}(\tau) := \frac{d^\alpha f(\tau)}{d\tau^\alpha} = \begin{cases} \dfrac{1}{\Gamma(-\alpha)}\displaystyle\int_0^\tau (\tau-\xi)^{-\alpha-1}(f(\xi)-f(0))d\xi, & \alpha < 0, \\[2ex] \dfrac{1}{\Gamma(1-\alpha)}\dfrac{d}{d\tau}\displaystyle\int_0^\tau (\tau-\xi)^{-\alpha}(f(\xi)-f(0))d\xi, & 0 < \alpha < 1, \\[2ex] \dfrac{d^l(f^{(\alpha-l)}(\tau))}{d\tau^l}, & l \leq \alpha < l+1, \end{cases} \tag{6}$$

wherein $\Gamma(\cdot)$ is the function of Gamma and l shows a positive integer. The case $0 < \alpha < 1$ in (6) is used in the model (1). Moreover, the Caputo fractional derivative is expressed by [13]:

$$_0^C D_\tau^\alpha f(\tau) = (\Gamma(1-\alpha))^{-1}\int_0^\tau (\tau-\xi)^{-\alpha}f'(\xi)d\xi, \quad 0 < \alpha < 1. \tag{7}$$

Pseudospectral (PS) solvers can be seen as generalizations of the FD methods that can result in higher accuracies using a lower number of discretization points. One such scheme has recently been developed in [14] for pricing the multi-asset option pricing problem, which is based on Chebyshev roots for discretization of the domain adaptively.

However, next to the PS methods, there is a category of methods that are less sensitive to the computational domain. In fact, radial basis function (RBF) methods are an important portion part of meshless methods. Global and local meshless RBF methods, which lead to full and sparse matrices, respectively, are two important divisions of such methods [15]. Another approach with good results that inherits both from FD and the RBF methods is the localized RBF–FD method [16].

It is known that FD stencils obtain accuracy orders in proportion to their stencil widths. Note that the existence, uniqueness, and convergence of the RBF approximations were argued in detail at [17]. RBF–FD methods [16] are essentially a generalization of the classic FD method, which has successfully been employed to numerically solve a variety of PDE problems.

The inverse multi quadric (IMQ) RBF is defined by

$$\phi(r_i) = \frac{1}{\sqrt{c^2 + r_i^2}}, \qquad i = 1, 2, \ldots, N, \tag{8}$$

where the parameter of shape is c and $r_i = \|s - s_i\|$ shows the Euclidean distance. The nonzero parameter c plays a key role in the accuracy of approximations ([15] Chapter 15.5).

The work [18] investigated the discretization of the time fractional variable of (1) first, then employed a multi-quadric RBF to fully discretize the financial model, and then obtained the accuracy of order $2 - \alpha$ in the case of smooth solutions. Another mesh-free scheme based on the RBF pseudo-spectral (PS) approach was discussed to solve (1) in [19].

Here, it is necessary to note that in several works in the literature such as [20], first, some logarithmic transformation is employed in the spatial domain of (1) to derive a constant-coefficient version of (1) in order to then construct a method on it. This is not pursued in this work since such transformations are mainly faced with the logarithm of zero, which is not defined, and thus smaller truncated domains should be considered. The authors of work [21] investigated how much the choice of the shape parameter can affect the accuracy of the RBF meshless methods in solving the fractional Black–Scholes PDEs and proposed a procedure to find a good shape parameter for such a purpose.

Motivated by the works [22,23], the goal of this paper is to price European options by providing advantages to solving (1) without imposing any logarithmic transformation, as well as by transforming the whole continuous problem into a set of linear algebraic equations.

The remaining parts are organized as follows. In Section 2, the discretzation along the time-fractional derivative is provided, which works for both uniform and non-uniform meshes. Then, in Section 3 the spatial discretization for the Black–Scholes model is provided with an emphasis on the hot area at which the initial condition of the PDE problem has discontinuity. In fact, the fractional PDE problem in this work has non-smoothness at $s = E$. Next, in Section 4, the numerical treatment for pricing options under the time-fractional Black–Scholes model is proposed in detail. It is attempted to propose the new scheme in matrix environment to minimize the computational burdensome and increase the efficiency of the proposed scheme. Thence, Section 5 is provided to discuss the applicability and usefulness of the contributed formulas in practice. Several comparisons are worked out along with numerical simulations. Finally, the conclusion is provided in Section 6.

2. Temporal Discretization

In this section, we provide a version of the L1 scheme for approximating the time-fractional derivative. Now, assume that

$$0 = \tau_0 < \tau_1 < \cdots < \tau_n = T, \tag{9}$$

is a set of nodes in $[0, T]$ with the uniform temporal step size $\Delta\tau$. Diethelm, in [24], proposed the following L1 scheme to compute the RL fractional derivative when $0 < \alpha < 1$, with f being a sufficiently smooth function:

$$
{}_0^R D_\tau^\alpha(f(\tau_n)) = \Delta\tau^{-\alpha} \sum_{j=0}^n w_{j,n} f(\tau_{n-j}) + \mathcal{O}(\Delta\tau^{2-\alpha}),
\tag{10}
$$

where

$$
\Gamma(2-\alpha)w_{j,n} = \begin{cases}
-j^{1-\alpha} + (j-1)^{1-\alpha}, & j = n, \\
(j+1)^{1-\alpha} + (j-1)^{1-\alpha} - 2j^{1-\alpha}, & j = 1, 2, \ldots, n-1, \\
1, & j = 0.
\end{cases}
\tag{11}
$$

The following identity is mainly being used when solving time-fractional PDEs [25]:

$$
{}_0^R D_\tau^\alpha(f(\tau) - f(0)) = {}_0^C D_\tau^\alpha f(\tau).
\tag{12}
$$

On uniform meshes, the L1 scheme is provided in another version as follows :

$$
\begin{aligned}
{}_0^C D_\tau^\alpha(v(s_i, \tau_{k+1})) &= \frac{1}{\Gamma[2-\alpha]} \sum_{j=0}^k \frac{v_{i,j+1} - v_{i,j}}{\Delta\tau} \\
&\quad \times \left((k+1-j)^{1-\alpha}\Delta\tau^{1-\alpha} - (k+1-j-1)^{1-\alpha}\Delta\tau^{1-\alpha} \right), \\
&= \frac{1}{\Gamma[2-\alpha]} \sum_{j=0}^k \frac{v_{i,j+1} - v_{i,j}}{\Delta\tau} \Delta\tau^{1-\alpha} \left((k+1-j)^{1-\alpha} - (k-j)^{1-\alpha} \right), \\
&= \frac{\Delta\tau^{-\alpha}}{\Gamma[2-\alpha]} \sum_{j=0}^k \frac{v_{i,j+1} - v_{i,j}}{\Delta\tau} \left((j+1)^{1-\alpha} - (j)^{1-\alpha} \right).
\end{aligned}
\tag{13}
$$

This uses a nonuniform piecewise linear approximation to attain a $(2 - \alpha)$ convergence rate for the α-order fractional derivative.

3. The IMQ Function for Spatial Discretization

The truncated spatial domain for (1) is provided by $\Omega = [0, s_{\max}]$, where $s_{\max}$ is a positive parameter that is large enough to minimize the incorporation of boundary conditions and the domain truncation. To furnish a mesh, some strategies have already been provided in [26]. Similarly, assume that $\{s_i\}_{i=1}^m$ is a partition for $s \in [s_{\min}, s_{\max}]$. Then, we consider

$$
s_i = \Psi(\vartheta_i), \qquad 1 \le i \le m,
\tag{14}
$$

where $m \gg 1$ and

$$
\vartheta_{\max} = \vartheta_m > \cdots > \vartheta_2 > \vartheta_1 = \vartheta_{\min},
\tag{15}
$$

are m equally-spaced nodes having features as follows:

$$
\begin{aligned}
\vartheta_{\min} &= \sinh^{-1}\left(\frac{s_{\min} - s_{\text{left}}}{d_1} \right), \\
\vartheta_{\text{int}} &= \frac{s_{\text{right}} - s_{\text{left}}}{d_1}, \\
\vartheta_{\max} &= \vartheta_{\text{int}} + \sinh^{-1}\left(\frac{s_{\max} - s_{\text{right}}}{d_1} \right).
\end{aligned}
\tag{16}
$$

We also take into account that $s_{\min} = 0$ and $s_{\max} = 3E$. The parameter $d_1 > 0$ controls the density of the nodes around $s = E$. In addition, one defines

$$
\Psi(\vartheta) = \begin{cases}
s_{\text{left}} + d_1 \sinh(\vartheta), & \vartheta_{\min} \leq \vartheta < 0, \\
s_{\text{left}} + d_1 \vartheta, & 0 \leq \vartheta \leq \vartheta_{\text{int}}, \\
s_{\text{right}} + d_1 \sinh(\vartheta - \vartheta_{\text{int}}), & \vartheta_{\text{int}} < \vartheta \leq \vartheta_{\max}.
\end{cases} \tag{17}
$$

A common choice for the free parameter in (16) is $d_1 = \frac{E}{10}$, while $s_{\text{left}} = \max\{0.5, e^{-0.0025T}\} \times E$, $s_{\text{right}} = E$, and $[s_{\text{left}}, s_{\text{right}}] \subset [0, s_{\max}]$. Here, $d_1 = \frac{E}{10}$.

Now, consider a mesh of interior nodes with m scattered nodes $s_1, s_2, \ldots, s_m$, and a differential operator $L[\cdot]$. For the grid point $s = s_j$, now the goal is to approximate $Lv(s_j)$ with a linear combination of the values of v at the m nodes to obtain the following:

$$
L[v(\mathbf{s}_j)] \simeq \sum_{i=1}^{m} \alpha_i v(\mathbf{s}_i), \tag{18}
$$

where α_i are the weighting coefficients [27].

For the 1st derivative, we consider a mesh of three non-uniform points as $[s_i - h, s_i, s_i + \kappa h]$, $(\kappa > 0, h > 0)$. Now, one can write that

$$
v'(s_i) \simeq \Xi_1 v(s_{i-1}) + \Xi_2 v(s_i) + \Xi_3 v(s_{i+1}). \tag{19}
$$

Using the RBFs in (19) centered at $s_{i-1} = s_i - h$, s_i, and $s_{i+1} = s_i + \kappa h$, yields the coefficients when $c \gg h$ as follows [27]:

$$
\begin{aligned}
\Xi_1 &= -\frac{\kappa(4c^2 + h^2(5\kappa + 1))}{4c^2 h(\kappa + 1)}, \\
\Xi_2 &= \frac{(\kappa - 1)(4c^2 + 5h^2\kappa)}{4c^2 h\kappa}, \\
\Xi_3 &= \frac{4c^2 + h^2\kappa(\kappa + 5)}{4c^2 h\kappa(\kappa + 1)}.
\end{aligned} \tag{20}
$$

For computing the weights for the function's 2nd derivative, one can write

$$
v''(s_i) \simeq \Theta_1 v(s_{i-1}) + \Theta_2 v(s_i) + \Theta_3 v(s_{i+1}). \tag{21}
$$

As long as $h \ll c$, it is possible to find the following weights:

$$
\begin{aligned}
\Theta_1 &= \frac{4c^2 + h^2(\kappa(13 - 5\kappa) + 1)}{2c^2 h^2(\kappa + 1)}, \\
\Theta_2 &= \frac{h^2(\kappa(5\kappa - 19) + 5) - 4c^2}{2c^2 h^2 \kappa}, \\
\Theta_3 &= \frac{4c^2 + h^2(\kappa(\kappa + 13) - 5)}{2c^2 h^2 \kappa(\kappa + 1)}.
\end{aligned} \tag{22}
$$

4. Numerical Implementation

Up to now, we have obtained a strategy for discretization along a time-fractional derivative in Section 2 and designed new weights for applying the RBF–FD methodology in order to solve the PDE model along space in Section 3.

Again, by denoting

$$
v_{i,j} \simeq v(s_i, \tau_j), \tag{23}
$$

we are now able to write down the whole discretization procedure of (1) in the European case, as follows:

$$D_\tau^\alpha v(s_i, \tau_{j+1}) + \mathcal{O}(\Delta\tau_{\max}^{2-\alpha}) = \frac{1}{2}\sigma^2 s_i^2 [\Theta_{i-1,j}v_{i-1,j} + \Theta_{i,j}v_{i,j} + \Theta_{i+1,j}v_{i+1,j}] + \mathcal{O}(h_{\max})$$
$$+ (r-q)s_i[\Xi_{i-1,j}v_{i-1,j} + \Xi_{i,j}v_{i,j} + \Xi_{i+1,j}v_{i+1,j}] + \mathcal{O}(h_{\max}^2) \tag{24}$$
$$- rv_{i,j},$$

wherein $\Delta\tau_{\max}$ and $h_{\max}$ are the maximum of the step sizes along space and time; furthermore, we have

$$D_\tau^\alpha v(s_i, \tau_{j+1}) = \frac{1}{\Gamma[2-\alpha]} \sum_{g=0}^{j} \frac{v_{i,g+1} - v_{i,g}}{\Delta\tau_{g+1}} \left((\tau_{j+1} - \tau_g)^{1-\alpha} - (\tau_{j+1} - \tau_{g+1})^{1-\alpha} \right). \tag{25}$$

We re-write our proposed procedure scheme in matrix notations. Let us first define two differentiation matrices having the weights for the IMQ RBF–FD procedure described in Section 3 in what follows:

$$\mathfrak{D}_s = \begin{cases} \Xi_{i,j} \text{ using (20)} & |j - i| \leq 1, \\ 0 & \text{otherwise,} \end{cases} \tag{26}$$

and

$$\mathfrak{D}_{ss} = \begin{cases} \Theta_{i,j} \text{ using (22)} & |j - i| \leq 1, \\ 0 & \text{otherwise.} \end{cases} \tag{27}$$

For the discretization nodes located on the boundaries, we point out that the relations (20) and (22) are useful for the rows 2 to $m-1$, while for the first and last rows of the derivative matrices (26) and (27), the weighting coefficients might not be useful on boundaries and thus sided estimations must be imposed. This is the procedure for constructing the weights possessing the second order (three nodes for approximating the 1st derivative $\{s_1, s_2, s_3\}$):

$$f'(s_1) = f[s_1, s_2] + f[s_1, s_3] - f[s_3, s_2] + \mathcal{O}\left((s_1 - s_2)^2\right), \tag{28}$$

and

$$f'(s_m) = -f[s_{m-1}, s_{m-2}] + f[s_{m-2}, s_m] + f[s_{m-1}, s_m] + \mathcal{O}\left((s_m - s_{m-1})^2\right), \tag{29}$$

where $f[y, o] = (f(y) - f(o))/(y - o)$. In a similar way, we can write the nonuniform second-order approximations for the second derivative on the boundary nodes. However, the weights obtained for such nodes do not affect the final results since, after the incorporation of the boundary conditions, these weights are replaced by boundary conditions.

Let us denote $\mathcal{D}_\tau$ as the matrix of differentiation along time, while $\otimes$ denotes the Kronecker product. To construct our final localized method for fractional European options, we proceed by the following system matrix Y:

$$Y = \frac{1}{2}\sigma^2 \mathbf{S}^2 (\mathfrak{D}_{ss} \otimes I_\tau) + (r-q)\mathbf{S}(\mathfrak{D}_s \otimes I_\tau) - rI_N, \tag{30}$$

wherein

$$I_N = I_s \otimes I_\tau, \tag{31}$$

is an $N \times N$ unit matrix, with I_s and I_τ being $m \times m$ and $n \times n$ unit matrices, respectively. The matrix Y has a block tri-diagonal structure. Here, the diagonal matrix **S** is also provided below:

$$\mathbf{S} = \text{diag}(s_1, s_2, \cdots, s_m) \otimes I_\tau. \tag{32}$$

Therefore, the fractional BS model (24) under $0 < \alpha < 1$ can be fully discretized as follows:

$$(I_s \otimes \mathcal{D}_\tau)V = YV, \tag{33}$$

where $V = (v_{1,1}, v_{1,2}, \ldots, v_{m,n})^*$. On the other hand, by considering

$$\mathcal{A} = (I_s \otimes \mathcal{D}_\tau) - Y, \tag{34}$$

we obtain $\mathcal{A}V = 0$, and now by imposing the initial and boundary conditions, we have the following set of linear algebraic equations of size $N \times N$:

$$\bar{A}V = \bar{\mathfrak{b}}, \tag{35}$$

where $\bar{A}$ and $\bar{\mathfrak{b}}$ are, respectively, the system matrix and system vector, after imposing the boundaries and the initial conditions. Here, $\bar{A}$ is a non-zero, real, un-symmetric, and sparse system matrix. The set of Equation (35) is well-posed, i.e., there exists a unique solution since $\bar{A}$ is an invertible matrix, and therefore the constructed difference scheme has a unique solution.

Combining what we obtained with the nonuniform approximation of the fractional derivative and the use of Kronecker product to achieve sparse matrices results in an efficient solution for pricing (1).

We remark that although in this work we have focused on solving the financial model (1), the weights and procedure proposed can be used and extended in a similar manner for other types of financial PDEs in option pricing.

Theorem 1. *Let $\sigma, r > 0$, $q \geq 0$, $c \gg h$ and $s_{\max}$ be an enough large scalar to truncate the spatial domain. If the spatial discretization is uniform, then the proposed RBF–FD scheme with a uniform mesh for solving the financial model (1) is unconditionally time-stable.*

Proof. To prove this, let us first write the first temporal step that we employ to proceed after imposing all the necessary initial and boundary conditions as follows:

$$(\mathcal{D}_\tau[[2,2]]I_s - A)\text{payoff}[2] = \text{payoff}[1]. \tag{36}$$

Since all of the eigenvalues of A are negative-definite and subsequently the eigenvalues of $-A$ are positive definite, we obtain that no eigenvalues of $(\mathcal{D}_\tau[[2,2]]I_s - A)$ are vanishing (after imposing the boundaries). Note that here by using the Mathematica notations, payoff$[i]$, $i = 1, 2, \ldots, n$ stands for the solutions as vectors per time step, i.e., payoff$[1]$ is the initial condition, and after that we obtain the solution vectors and put them in payoff$[i]$.

Now, we have $\mathcal{D}_\tau[[2,2]] > 0$ and thus Det $(\mathcal{D}_\tau[[2,2]]I_s - A) \neq 0$, whose states are invertible, and there is a unique solution at this step . By mathematical induction and the structure of the proposed method, this can be deduced for the whole solution method regardless of $\Delta\tau_{\max}$.

Now, to show the unconditional stability and by a similar spirit of logic, it is enough to state that all eigenvalues of $(\mathcal{D}_\tau[[2,2]]I_s - A)^{-1}$ have a modulus less than or equal to one. This is always valid since the following inequality holds:

$$|(\mathcal{D}_\tau[[2,2]] - \lambda_i)| \geq 1, \qquad i = 1, 2, \ldots, m, \tag{37}$$

where λ_i are the eigenvalues of A. For the general case again by way of mathematical induction, it is enough to state that

$$\rho((d_{j,j}I_s - A)^{-1}) \leq 1, \tag{38}$$

which is true since $\lambda_{\min}(d_{j,j}I_s - A) = 1$. The proof ends now. □

The convergence of the mesh-free method is independent of the convergence order of the L1 scheme along the time variable.

5. Computational Aspects

This section concerns illustrations of the existing solver and the new efficient method for pricing financial options . The compared methods on the same uniform temporal meshes are

- The FD method proposed in [28] denoted by FD2.
- The proposed method described in Section 4 denoted by PM based on an adaptive mesh in Section 3.

We do not compare our results with other numerical methods in the literature since in most of them a source function was added to the PDE model (1) in order to furnish a theoretical solution for the model. This action is meaningless in terms of mathematical finance. All computations and programs were written in the programming package Mathematica 12.0.

All the compared methods here are written in the programming package Mathematica 12.0 [29]. The CPU time is reported in seconds denoted T_{Method}.

The absolute error is computed by

$$\varepsilon = \left| v_{\text{approx}}(s, \tau) - v_{\text{ref}}(s, \tau) \right|, \tag{39}$$

wherein v_{ref} and v_{approx} are the referenced and numerical solutions, respectively.

We also check the computational order of convergence (COC) of various methods by employing the fact that if $v_{\text{approx}} = v_{\text{exact}} + \mathcal{O}(\Delta \tau^p)$, then one can approximate the exponent p, i.e., COC, as follows [30]:

$$p \approx \left| \log_2 \frac{v_{\text{approx}}(4n+1) - v_{\text{approx}}(2n+1)}{v_{\text{approx}}(2n+1) - v_{\text{approx}}(n+1)} \right|, \tag{40}$$

where $v_{\text{approx}}(2n+1)$ means the obtained approximated solution with $2n+1$ nodes along time, and similarly for the others.

An efficient way can be employed here for the selection of the shape parameter in experiments, as follows:

$$c = 4 \max\{\Delta s_i\}, \quad 1 \le i \le m - 1, \tag{41}$$

where Δs_i are the increments along s variable mesh. This is mainly based on the existing discussion provided in [27]. In this way, the parameter of shape is chosen adaptively based on the size of the mesh and its step size.

Example 1. *A European call case is compared by having the settings below:*

$$r = 5\%, \ T = 1 \ year, \ q = 0, \ E = 100\$, \ \sigma = 40\%, \ \alpha = 0.8. \tag{42}$$

The reference solution is $v(E, T) \simeq 18.1883$.

The simulation results for this experiment are shown in Table 1. The numerical solutions based on FD2 and PM are portrayed in Figures 1 and 2.
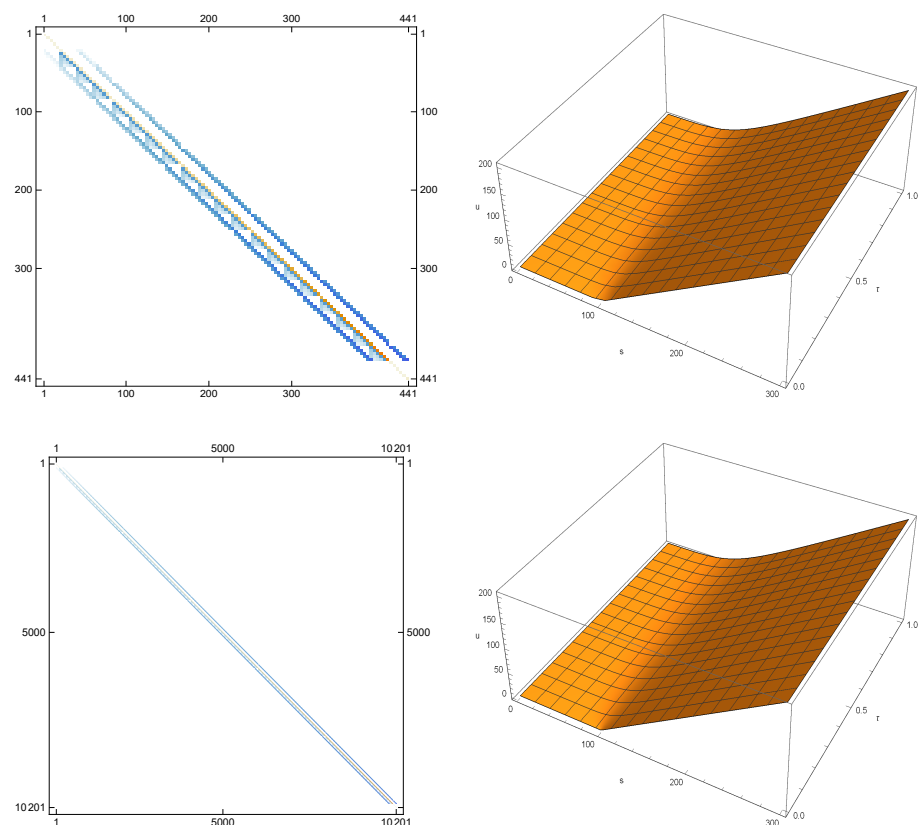
To re-check the numerical rate of convergence, here we use (40) and report the COCs in Table 2 when $m = 40$ is fixed and the number of temporal discretization nodes gets doubled each time. The results agree with the theoretical discussions.

Table 1. Numerical results of fractional European call option pricing under Test Problem 1.

m,n	v_{FD2}	ε_{FD2}	T_{FD2}	v_{PM}	ε_{PM}	T_{PM}
10	16.070	2.11×10^{0}	0.01	17.378	8.10×10^{-1}	0.01
20	17.889	2.98×10^{-1}	0.02	17.694	4.94×10^{-1}	0.02
40	17.913	2.75×10^{-1}	0.16	18.003	1.85×10^{-1}	0.18
80	18.039	1.48×10^{-1}	3.96	18.213	2.46×10^{-2}	3.84
120	18.055	1.33×10^{-1}	20.02	18.190	1.64×10^{-3}	20.96

Table 2. Temporal COCs for different schemes under Test Problem 1.

Scheme ↓, n →	5 + 1	10 + 1	20 + 1	40 + 1	80 + 1	160 + 1	Mean ↓
FD2 (Price)	17.346	17.664	17.830	17.915	17.958	17.981	
ε_{FD2}	8.4×10^{-1}	5.2×10^{-1}	3.5×10^{-1}	2.7×10^{-1}	2.3×10^{-1}	2.0×10^{-1}	
FD2 (COC)	-	-	0.94	0.96	0.97	0.97	0.9
PM (Price)	17.298	17.526	17.890	18.021	18.107	18.134	
ε_{PM}	8.9×10^{-1}	6.6×10^{-1}	2.2×10^{-1}	1.6×10^{-2}	8.1×10^{-2}	5.4×10^{-2}	
PM (COC)	-	-	0.83	0.97	1.07	1.11	1.0

Figure 1. Numerical results in Test Problem 1 for FD. (**Top Left**) The sparsity pattern of the coefficient matrix in (35) based on $m = n = 21$. (**Top Right**) Time fractional option pricing curve. (**Bottom Left**) The sparsity pattern of the coefficient matrix in (35) based on $m = n = 101$. (**Bottom Right**) Time fractional option pricing curve.
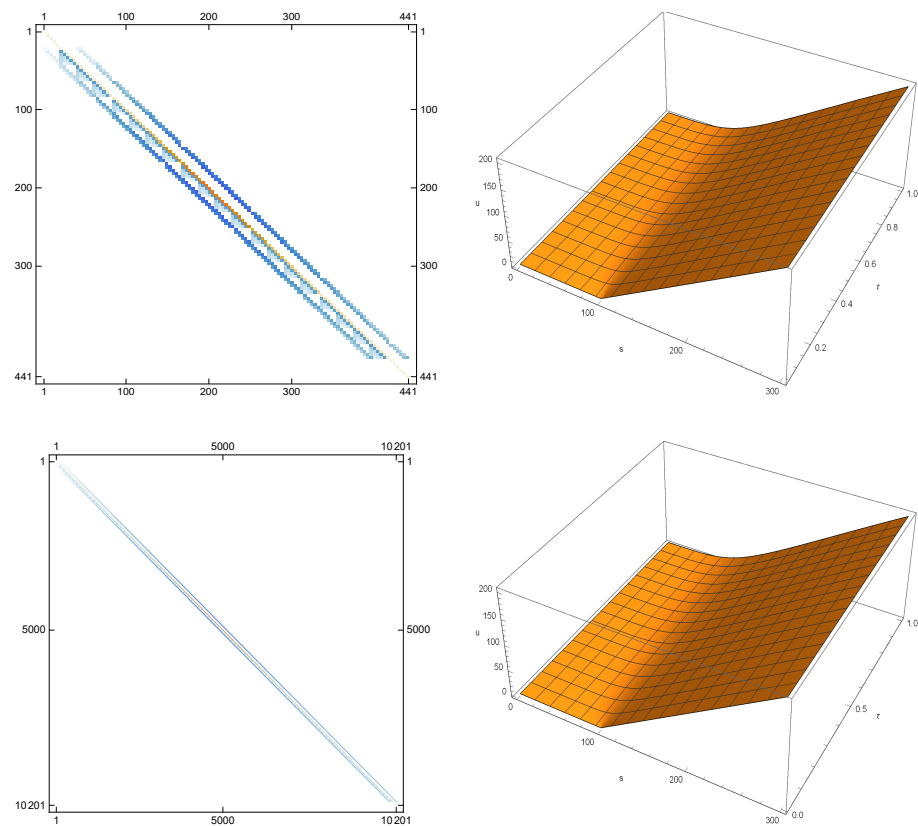
Figure 2. Numerical results in Test Problem 1 for PM. (**Top Left**) The sparsity pattern of the coefficient matrix in (35) based on $m = n = 21$. (**Top Right**) Time fractional option pricing curve. (**Bottom Left**) The sparsity pattern of the coefficient matrix in (35) based on $m = n = 101$. (**Bottom Right**) Time fractional option pricing curve.

Example 2. *A European put case with the following settings is evaluated and compared:*

$$E = 100\$, \ r = 5\%, \ T = 2 \ year, \ q = 20\%, \ \sigma = 30\%, \ \alpha = 0.7. \qquad (43)$$

The reference solution is $v(E, T) \simeq 24.6299$. The results of comparisons for this case are provided in Table 3, which shows the fast convergence as well as the stable behavior of PM in contrast to the fundamental method FD2. The numerical rates of convergence are also reported in this case, showing this rate for the whole numerical procedure. Additionally, to check the behavior of the numerical solutions by varying the time-fractional derivative, Figure 3 is provided to re-illustrate this.

In fact, we have taken the fractional parameter as 0.8 in Example 1 and 0.7 in Example 2, to reveal when α approaches 1; then, the fractional PDE's solution approaches the classical integer order case.

Table 3. Computational reports of fractional European put option pricing under Test Problem 2.

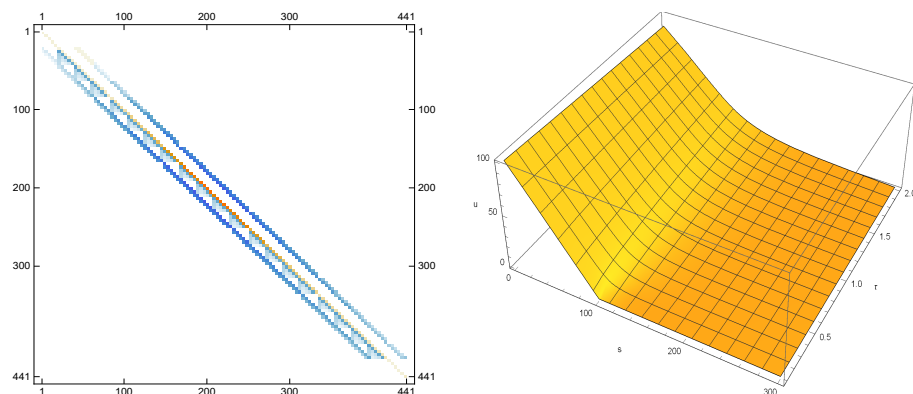| m,n	v_{FD2}	ε_{FD2}	T_{FD2}	p_{FD2}	v_{PM}	ε_{PM}	T_{PM}	p_{PM}
11	23.914	7.1×10^{-1}	0.01	-	23.631	9.9×10^{-1}	0.03	-
21	24.316	3.1×10^{-1}	0.03	-	24.117	5.1×10^{-1}	0.05	-
41	24.466	1.6×10^{-1}	0.15	1.42	24.356	2.7×10^{-1}	0.21	1.21
81	24.545	8.4×10^{-2}	4.14	0.92	24.565	6.4×10^{-2}	4.69	1.30
161	24.580	4.9×10^{-2}	63.97	1.17	24.636	6.1×10^{-3}	64.01	1.31

Figure 3. Numerical results in Test Problem 2 for PM based on $m = n = 21$. (**Left**) The sparsity pattern of the coefficient matrix in (35). (**Right**) Time fractional option pricing curve.

6. Concluding Summary

It is well-known that the BS PDE could not be employed in some circumstances due to several restrictions. On the other hand, the most important merit in employing fractional derivatives in PDE models lies in their nonlocal property since integer-order differential operators are local operators. This feature can be employed in order to obtain better predictions for option prices.

Accordingly, in this work we concentrated on the time-fractional BS PDE with non-constant coefficients under the non-smooth initial conditions and contributed a scheme for solving this PDE efficiently. Toward this purpose, a procedure based on nonuniform discretization along space was presented. The concentration of the graded meshes for this aim is to focus near zero along time and on the strike price along space. The application of non-uniform meshes along the asset price for the time-fractional BS model was carried out in this work for the first time. Then, the RBF–FD scheme based on the IMQ was studied and its weights were introduced. The continuous time-fractional problem was transformed into solving a set of linear algebraic equations. The convergence of the scheme was discussed as well. Numerical experiments were provided to support the theoretical discussions and confirm that the new method is efficient for option pricing under the fractional BS model.

References

1. Soleymani, F.; Akgül, A. Asset pricing for an affine jump-diffusion model using an FD method of lines on non-uniform meshes. *Math. Methods Appl. Sci.* **2019**, *42*, 578–591. [CrossRef]
2. Seydel, R.U. *Tools for Computational Finance*, 6th ed.; Springer: London, UK, 2017.
3. Wyss, W. The fractional Black–Scholes equation. *Fract. Calc. Appl. Anal.* **2000**, *3*, 51–62.
4. Hurst, H.E. Long-term storage capacity of reservoirs. *Trans. Am. Soc. Civ. Eng.* **1951**, *116*, 770–799. [CrossRef]

5. Soheili, A.R.; Soleymani, F. Some derivative-free solvers for numerical solution of SODEs. *SeMA J.* **2015**, *68*, 17–27. [CrossRef]
6. Soheili, A.R.; Amini, M.; Soleymani, F.; A family of Chaplygin-type solvers for Itô stochastic differential equations. *Appl. Math. Comput.* **2019**, *340*, 296–304. [CrossRef]
7. Cutland, N.J.; Kopp, P.E.; Willinger, W. Stock price returns and the Joseph effect: A fractional version of the Black–Scholes model, In *Progress in Probability, Proceedings of the Former Ascona Conferences on Stochastic Analysis, Random Fields and Applications*; Birkhauser: Basel, Switzerland, 1995; Volume 36, pp. 327–351.
8. Norros, I.; Valkeila, E.; Virtamo, J. A Girsanov-type formula for the fractional Brownian motion. In Proceedings of the First Nordic-Russian Symposium on Stochastics, Helsinki, Finland, August 1996.
9. Jumarie, G. Derivation and solutions of some fractional Black–Scholes equations in coarse-grained space and time: Application to Merton's optimal portfolio. *Comput. Math. Appl.* **2010**, *59*, 1142–1164. [CrossRef]
10. Awasthi, A.; Tk, R. An accurate solution for the generalized Black–Scholes equations governing option pricing. *AIMS Math.* **2020**, *5*, 2226–2243. [CrossRef]
11. Lo, A. Long-term memory in stock market prices. *Econometrica* **1991**, *59*, 1279–1313. [CrossRef]
12. Jumarie, G. Modified Reimann-Liouville derivative and fractional Taylor series of non-differentiable functions further results. *Comput. Math. Appl.* **2006**, *51*, 1367–1376. [CrossRef]
13. Caputo, M. Linear model of dissipation whose Q is almost frequency independent. II. *Geophys. J. Int.* **1967**, *13*, 529–539. [CrossRef]
14. Soleymani, F. Pricing multi-asset option problems: A Chebyshev pseudo-spectral method. *BIT Numer. Math.* **2019**, *59*, 243–270. [CrossRef]
15. Fasshauer, G.E. *Mesh-Free Approximation Methods with Matlab*; World Scientific Publishing Co.: Singapore, 2007.
16. Tolstykh, I. On using RBF-based differencing formulas for unstructured and mixed structured-unstructured grid calculation. In Proceedings of the 16th IMACS World Congress, Lausanne, Switzerland, 21–25 August 2000; Volume 228, pp. 4606–4624.
17. Franke, C.; Schaback, R. Convergence order estimates of meshless collocation methods using radial basis functions. *Adv. Comput. Math.* **1998**, *8*, 381–399. [CrossRef]
18. Nikan, O.; Avazzadeh, Z.; Tenreiro Machado, J.A. Localized kernel-based meshless method for pricing financial options underlying fractal transmission system. *Math. Methods Appl. Sci.* **2021**. [CrossRef]
19. Golbabai, A.; Nikan, O.; Nikazad, T. Numerical analysis of time fractional Black–Scholes European option pricing model arising in financial market. *Comput. Appl. Math.* **2019**, *38*, 173. [CrossRef]
20. Golbabai, A.; Nikan, O. A computational method based on the moving least-squares approach for pricing double barrier options in a time-fractional Black–Scholes model. *Comput. Econ.* **2020**, *55*, 119–141. [CrossRef]
21. Haq, S.; Hussain, M. Selection of shape parameter in radial basis functions for solution of time-fractional Black–Scholes models. *Appl. Math. Comput.* **2018**, *335*, 248–263. [CrossRef]
22. Torres-Hernandez, A.; Brambila-Paz, F.; Torres-Martínez, C. Numerical solution using radial basis functions for multidimensional fractional partial differential equations of type Black–Scholes. *Comput. Appl. Math.* **2017**, *40*, 1–25. [CrossRef]
23. Özdemir, N.; Yavuz, M. Numerical solution of fractional Black–Scholes equation by using the multivariate Padé approximation. *Acta Phys. Pol. A* **2017**, *132*, 1050–1053. [CrossRef]
24. Diethelm, K. An algorithm for the numerical solution of differential equations of fractional order. *Electron. Trans. Numer. Anal.* **1997**, *5*, 1–6.
25. Podlubny, I. *Fractional Differential Equations*; Academic Press: San Diego, CA, USA, 1999.
26. Kluge, T. Pricing Derivatives in Stochastic Volatility Models Using the Finite Difference Method. Ph.D. Thesis, TU Chemnitz, Chemnitz, Germany, 2002.
27. Soleymani, F.; Barfeie, M.; Khaksar Haghani, F. Inverse multi-quadric RBF for computing the weights of FD method: Application to American options. *Commun. Nonlinear Sci. Numer. Simul.* **2018**, *64*, 74–88. [CrossRef]
28. Zhang, H.; Liu, F.; Turner, I.; Yang, Q. Numerical solution of the time fractional Black–Scholes model governing European options. *Comput. Math. Appl.* **2016**, *71*, 1772–1783. [CrossRef]
29. Georgakopoulos, N.L. *Illustrating Finance Policy with Mathematica*; Springer International Publishing: London, UK, 2018.
30. Love, E.; Rider, W.J. On the convergence of finite difference methods for PDE under temporal refinement. *Comput. Math. Appl.* **2013**, *66*, 33–40. [CrossRef]